FOUNDATIONS OF CIVIL AND ENVIRONMENTAL ENGINEERING
No. 1 2002

Radoslaw L. Michalowski[1)], Ethan M. Dawson[2)]
[1)]University of Michigan, Ann Arbor, USA
[2)]URS Corp., San Francisco, USA

THREE-DIMENSIONAL ANALYSIS OF LIMIT LOADS ON MOHR-COULOMB SOIL

The bearing capacity of square and rectangular shallow footings is typically calculated using semi-empirical modifications of a strict solution to a strip footing over a weightless half-space. Two other approaches are presented in this paper for solving a problem of limit loads on a square footing. The kinematic approach of limit analysis is used first to arrive at the upper-bound solution, and the code *FLAC*^{3D} is utilized to obtain numerical results for an elasto-plastic soil. The results indicate that assumptions made in 3D limit analysis provide significant restrictions on the velocity fields. Consequently, numerical results based on the *FLAC*^{3D} code provide significantly lower, and therefore more accurate, limit loads.

Key words: soil mechanics, Mohr-Coulomb soil, limit load analysis

1. INTRODUCTION

The bearing capacity of shallow footings is a classical problem in foundation engineering, but practical calculations typically involve a modification of Prandtl [8] and Reissner [9] solutions to account for the footing shape, load inclination, and footing depth. This modification includes multiplying the components of the bearing capacity formula by respective coefficients, typically obtained from semi-empirical considerations. Two approaches are discussed in this paper for calculations of the bearing capacity of square footing. These calculations allow one to arrive at solutions to the shape factors used as modifiers in the classical bearing capacity formula.

Three-dimensional calculations based on the kinematic approach of limit analysis are rare because of difficulties associated with construction of non-trivial kinematically admissible velocity fields. A theoretical development is shown first to indicate that elaborate computations of the internal work rate in

ISSN 1642-9303

the volume of the mechanism and on kinematic discontinuities can be replaced with a surface integral that is less complicated to evaluate. These considerations are shown in the next section, followed by the description of the collapse mechanisms used in the analysis. Program *FLAC*^{3D} will be described next, and the results of computations using both methods will be presented. The paper will be concluded with final remarks.

2. LIMIT ANALYSIS OF SQUARE FOOTINGS

Although the method presented is valid for rectangular footings with an arbitrary aspect ratio, considerations are limited here to square footings. Construction of admissible velocity fields for plane-strain problems have led to reasonable upper-bound solutions to many engineering problems [1]. Non-trivial three-dimensional problems for frictional-cohesive soils, however, often lead to complex calculations where the internal work needs to be integrated over non-planar surfaces and within blocks with distributed shearing, leading to a loss of tractability.

It is assumed here that the soil yielding is described by the Mohr-Coulomb function, and the deformation is governed by the normality rule. Under these circumstances, the theorems of limit analysis are applicable. Calculations of the limit load are then carried out by constructing kinematically admissible collapse mechanisms, and equating the rate of internal work (also referred to as work dissipation) to the rate of work of external forces. The kinematic theorem of limit analysis states that the rate of work dissipation is not less that the rate of work of the external load in any kinematically admissible collase mechanism. Consequently, by equating the rate of internal work to external work, one can obtain the upper bound to an active limit load.

Becase the computations of internal work are elaborate for three-dimensional mechanisms, consideration is given in the next section to replacing these calculations with a simpler surface intergral.

2.1. Internal work

Unlike in elastic deformation processes, the shear and volumetric components of plastic deformation of frictional solids are related to one another. If the deformation of a pressure-dependent material is governed by the normality rule, then the ratio of the volumetric to the deviatoric strain rate uniquely follows from that flow rule. For instance, for the Mohr-Coulomb yield condition we have

$$\frac{\dot{\varepsilon}_v}{\dot{\gamma}_{\max}} = \frac{\dot{\varepsilon}_1 + \dot{\varepsilon}_3}{\dot{\varepsilon}_1 - \dot{\varepsilon}_3} = -\sin\phi \tag{2.1}$$

where the numerator represents the volumetric strain, the denominator is the maximum shear, and ϕ is the internal friction angle. The rate of internal work within a deforming volume can be calculated as

$$\dot{D} = (\dot{\varepsilon}_1 - \dot{\varepsilon}_3)\, c \cos\phi \tag{2.1}$$

where c is the soil cohesion. Utilizing Eq. (2.1) the rate of internal work now can be written as

$$\dot{D} = -\dot{\varepsilon}_v\, c \cot\phi = -(\dot{\varepsilon}_1 + \dot{\varepsilon}_3) c \cot\phi \tag{2.3}$$

Hence, the internal work can be represented as a function of the volumetric strain. Therefore, one might conjecture that the internal work in the entire mechanism can be calculated easily if the volumetric change in the entire velocity field is known.

Velocity fields used in the kinematic approach of limit analysis may include both the continuously deforming field and velocity discontinuities. The discontinuities can be interpreted as thin layers with continuous deformation in them, thus the consideration of internal work calculations will be carried out for a continuous deformation field only, without a loss of generality.

A method for estimation of the rate of the total volume change in the mechanism is indicated in the following. The total volumetric change in the entire mechanism can be expressed as

$$\int_V (\dot{\varepsilon}_1 + \dot{\varepsilon}_2 + \dot{\varepsilon}_3)\, dV = -\int_V \left(\frac{\partial v_1}{\partial x_1} + \frac{\partial v_2}{\partial x_2} + \frac{\partial v_3}{\partial x_3}\right) dV \tag{2.4}$$

where v_i is the velocity vector and V is the volume of the entire mechanism (the minus sign on the right-hand side comes from the compression-positive convention). Now using the divergence theorem we have

$$-\int_V \frac{\partial v_i}{\partial x_i}\, dV = -\int_S v_i n_i\, dS \tag{2.5}$$

where S is the entire surface surrounding volume V of the mechanism, and n_i is an outward unit vector normal to S. The total volumetric changes can thus be represented as a surface integral on the right-hand side of Eq. (2.5). The rate of the total internal work can be found by integration of Eq. (2.3), and, using Eq. (2.5), we obtain

$$\int_V \dot{D}(\dot{\varepsilon}_{ij})\, dV = -\int_V (\dot{\varepsilon}_1 + \dot{\varepsilon}_3)\, c \cot\varphi\, dV = \\ = \left(\int_{S_v} n_i\, v_i\, dS_v + \int_{S_t} n_i v_i\, dS_t \right) c \cot\varphi \tag{2.6}$$

Notice that the surface integral was decomposed here into an integral over boundary S_v where the velocity is given, and boundary S_t where the traction is given. Consequently, the rate of internal work within the volume of the incipient collapse mechanism can be replaced with a surface integral that is less complicated to compute. This method was used in the limit analysis approach presented here.

2.2. Mechanism of collapse

Early experimental tests on square and rectangular footings were performed by Golder [2], who indicated that the trace of the collapse mechanism on the soil surface resembles that in Fig. 1(a).

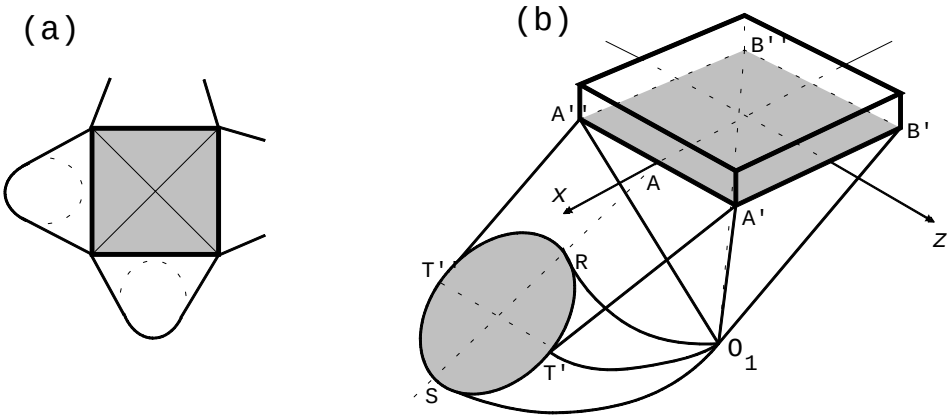

Fig. 1. Collapse mechanism with continuous deformation: (a) contour on the soil surface,
and (b) view of one section of the mechanism

The contours of a continuous mechanism consistent with that trace are shown in Fig. 1(b). To preserve the clarity of this mechanism, only one quarter of it is presented in Fig. 1(b). A tetrahedral block immediately beneath the footing moves down, and regions adjacent to the four flanks of the pyramid

(only one shown in Fig. 1) are separated from the soil at rest by non-linear conical surfaces.

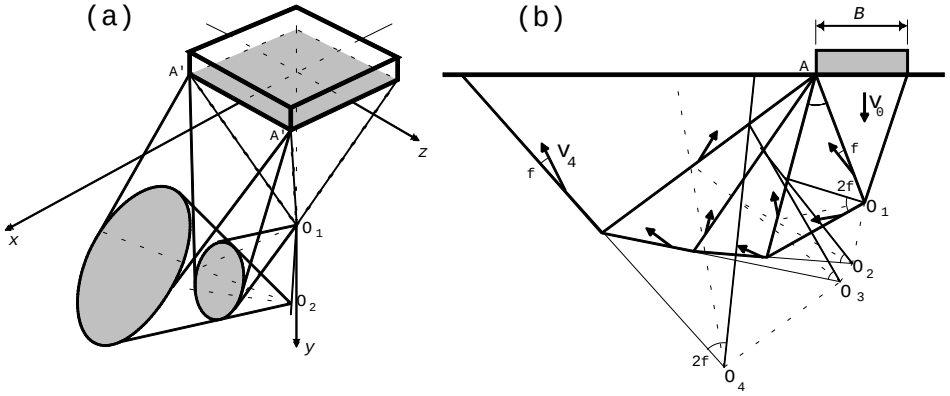

Fig. 2. Multi-block collapse mechanism: (a) view of a portion of the mechanism, and (b) cross section of the velocity

A multi-block mechanism is illustrated in Fig. 2. Both the continuous and the rigid-block mechanism are kinematically admissible and they both have been used in upper-bound calculations of limit loads on square footings. A more detailed discussion of these mechanisms is given in Michalowski [6].

It was surprizing to find out that the rigid-block mechanism led to the least upper bound, whereas the continuous mechanism led to a larger bearing capacity. It was also unexpected to find out that the mechanism associated with the best upper bound for square footings did not have diagonal symmetry, *i.e.*, the pyramid immediately underneath the footing, Fig. 2(a), had two triangular and two trapezoidal flanks. However, this is consistent with earlier findings of Shield and Drucker [10], who considered a smooth punch indentation problem of pressure-independent materials.

2.3. Results

The standard kinematic approach of limit analysis was used here to arrive at the limit loads on square and rectangular footings. We present here only limited results in terms of the bearing capacity factors N_c', N_q', and N_γ'. These factors are defined by the formula

$$p = c N_c' + q N_q' + \frac{1}{2}\gamma B N_\gamma' \tag{2.7}$$

where p is the average bearing traction beneath the footing. Coefficients N' in Eq. (2.7) include the influence of the footing shape. The results of computations

are presented in Table 1 for selected internal friction angle ϕ and footing aspect ratio *L/B*.

Table 1. Bearing capacity factors for selected ϕ and *L/B*

ϕ	*L/B* = 1			*L/B* = 2			*L/B* = 5		
	N_c'	N_q'	N_γ'	N_c'	N_q'	N_γ'	N_c'	N_q'	N_γ'
10°	12.66	3.23	0.77	10.73	2.89	0.97	9.36	2.65	1.07
20°	31.84	12.59	7.16	23.91	9.54	6.64	18.49	7.73	6.24
30°	104.01	61.05	59.89	67.09	39.73	46.20	45.84	27.4	36.9

As the results in Table 1 were obtained from the kinematic approach of limit analysis, they are not smaller than coefficients associated with a true solution.

3. NUMERICAL CALCULATIONS USING *FLAC*^{3D}

The second approach used here to estimate the bearing capacity of square footings is based on an elasto-plastic soil model, with the plastic behavior governed by the Mohr-Coulomb yield condition and the normality flow rule.

3.1. Program *FLAC*^{3D}

Bearing capacity computations were performed with the explicit finite difference code, *FLAC*^{3D} [3]. Although technically a finite difference program, *FLAC*^{3D} is similar to conventional displacement-method finite element programs. Element shape functions are used to construct a system of algebraic equations describing the relationship between nodal displacements and forces. However, in *FLAC*^{3D} this set of equations is solved by dynamic relaxation [7], an explicit time-marching procedure in which the full dynamic equations of motion are integrated step by step. Static solutions are obtained by including damping terms that gradually remove kinetic energy from the system. Although not a particularly fast algorithm, dynamic relaxation is simple and robust, and is particularly well suited for problems involving limit loads and steady plastic flow.

The *FLAC*^{3D} mesh is composed of eight-noded brick elements, subdivided into two overlapping sets of constant-strain tetrahedral elements. Volumetric strain rates are averaged over each set of tetrahedra to avoid the overconstraint

problems common in FEM plasticity formulations. This 'mixed discretization' scheme is described by Marti and Cundall [4].

3.2. Bearing capacity computations

Taking advantage of symmetry, only a quarter of the footing is modelled. Zero displacement is prescribed for all three components along the base of the mesh and along the two outer vertical boundaries (Fig. 3). Along the two inner vertical boundaries, representing symmetry planes, zero normal displacement is prescribed. For cases where the failure mechanism is relatively small (frictionless soil, smooth footing, or non-associative flow rule) a uniform mesh is used, 30 elements by 30 elements in the horizontal plane and 15 elements deep. For cases where the failure mechanism is relatively large, the element size is graded so that, using the same number of elements, the outer boundaries and base could be extended. For both meshes, the area representing the footing is 10 elements by 10 elements.

Bearing pressure is computed by applying a downward vertical displacement to nodes within the footing until a steady state load is reached. The reaction forces on the footing nodes are then summed and divided by the area of the footing.

3.3. Numerical results

Understandably, solving the punch-indentation problem for an elasto-plastic model is expected to yield limit loads that are lower than those from the upper-bound approach. Computations have not been made for a wide range of parameters, and only limited results are reported in Table 2.

It follows directly from comparing the results in Tables 1 and 2 that the upper-bound solution based on kinematic limit analysis overestimates the solution from *FLAC*^{3D} rather significantly. The upper-bound solutions to coefficients N_c' and N_q' for φ = 30° are roughly 70% larger than those for elasto-plastic solutions from *FLAC*^{3D}, and the coefficient N_γ' is threefold of that from *FLAC*^{3D}.

Table 2. Bearing capacity coefficients (rough square footings); *FLAC*^{3D} solutions

ϕ	N'_c	N'_q	N'_γ
30°	61.03	36.24	17.45

Preliminary calculations for other parameters indicate that the difference between the two solutions increases with an increase in the internal friction angle. To some extent, the large difference between the two solutions is surprising. For a plane-strain case (strip footings) the upper bound technique exactly matches the closed-form solutions to coefficients N_c and N_q [5]. The large overestimation for the 3-D case probably can be attributed to a significant constraint that the assumed three-dimensional geometry imposes on the deformation mechanism. In particular, the assumption of plane deformation within each of the four deformation regions (Fig. 1(a)) is likely to be responsible for the large difference. Of course, in the numerical solution for elasto-plastic soil no constraint is placed on deformation other than the kinematic boundary conditions and the material flow rule.

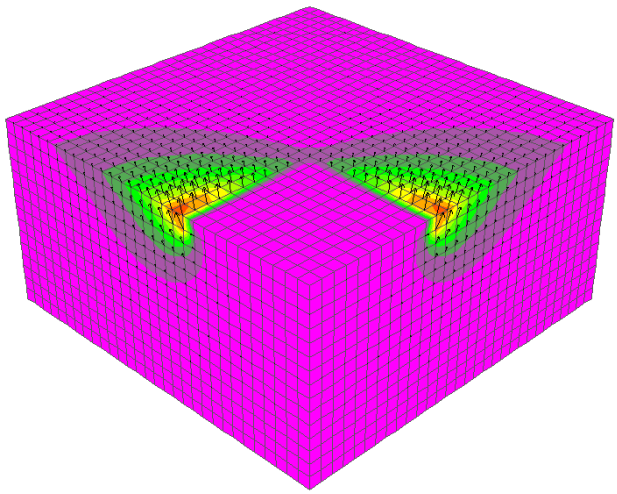

Fig. 3. Contours of total velocity magnitudes in the neighbourhood of a square footing (one quarter shown)

The above conjecture is supported by inspection of the velocity fields for the elasto-plastic solution. The graph in Fig. 3 presents contours of the velocity magnitudes in the neighbourhood of a rough square footing over a soil with an

internal friction angle of 30º and larger-than-zero unit weight. The gray scale in Fig. 3 indicates the ratio of the velocity magnitude to the footing velocity. The maximum of this ratio is 84, and the contour interval is 10 times the footing velocity.

An important characteristic of this deformation field is presented in Fig. 4. This top view of the displacement vectors indicates that the deformation is not plane in the regions adjacent to each side of the square footing. Limiting the mechanism to plane strain in the kinematic approach of limit analysis is likely to be responsible for the large overestimation in the upper-bound solutions.

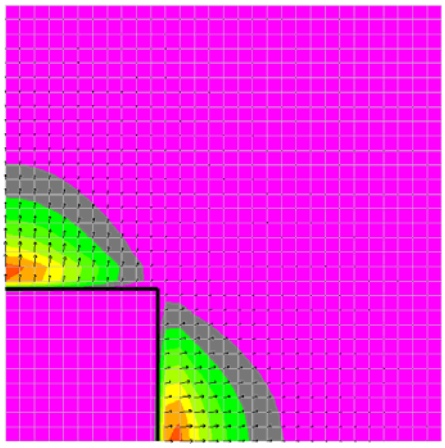

Fig. 4. Contours of the velocity magnitude at the soil surface

An interesting result in the kinematic approach is that the best upper bound was obtained from analysis based on a mechanism without diagonal symmetry rather than that in Fig. 1(a). A similar conclusion was obtained by Shield & Drucker [10] who obtained a closed-form solution for a smooth punch into metals (cohesive material). The coefficient N_c' from calculations with *FLAC*^{3D} for a smooth square punch is 5.43, as opposed to 5.71 from the limit analysis based on deformation consisting of four plane-strain regions [10]. The deformation field in an elasto-plastic soil beneath a smooth footing has four planes of symmetry, including two diagonal ones, Fig. 5. It appears that a lack of diagonal symmetry in the velocity field associated with the least upper-bound solution was an artifact of the mechanism used in the limit analysis.

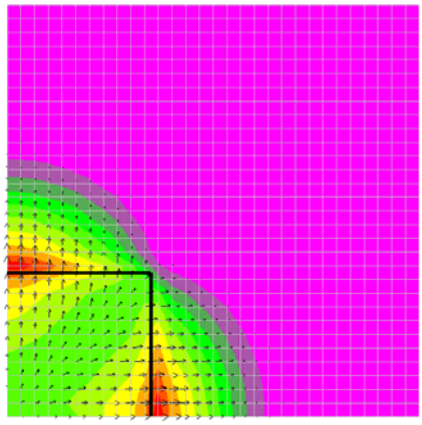

Fig. 5. Contours of the velocity magnitude at the soil surface for a smooth footing

4. FINAL REMARKS

Calculations using *FLAC*^{3D} remove some of the constraints characteristic of the kinematic approach of limit analysis where the 3D mechanism consists of four plane-strain regions. Numerical analysis with *FLAC*^{3D} leads to results for bearing capacity factors for square footings that are significantly lower than those from the upper-bound approach. The overestimation by limit analysis stems from a strict assumption of plane-strain deformation.

REFERENCES

1. Chen W.F.: Limit analysis and soil plasticity, Amsterdam, Elsevier 1975.
2. Golder H.Q.: The ultimate bearing pressure of rectangular footings, Journal of the Institution of Civil Engineers, **17**, 2, (1941) 161–174.
3. Itasca Consulting Group: FLAC^{3D}, Fast lagrangian analysis of continua in 3 dimensions, user's manual, Minneapolis, Minnesota, USA, 1997.
4. Marti J., Cundall P.: Mixed discretization procedure for accurate modelling of plastic collapse, Int. J. Numer. Analy. Meth. Geomech. **6** (1982) 129–139.
5. Michalowski R.L.: An estimate of the influence of soil weight on bearing capacity using limit analysis, Soils and Foundations, **37**, 4 (1997) 57–64.
6. Michalowski R.L.: Upper-bound load estimates on square and rectangular footings, Géotechnique, **51**, 9 (2001) 787–798.

7. Otter J. R. H., Cassell A. C., Hobbs R. E.: Dynamic relaxation (Paper No. 6986), Proc. Inst. Civil Eng., **35** (1966) 633–656.
8. Prandtl L.: Über die Härte plastischer Körper, Nachr. Königl. Ges. Wissensch., Göttingen, Mathematisch-physikalische Klasse (1920) 74–85.
9. Reissner H.: Zum Erddruckproblem, First Int. Congress for Applied Mechanics, eds. C.B. Biezeno, J.M. Burgers, Delft 1924, 295–311.
10. Shield R.T., Drucker D.C.: The application of limit analysis to punch-indentation problems, J. Appl. Mech., **20** (1953) 453–460.

R. L. Michalowski, E. M. Dawson

TRÓJWYMIAROWA ANALIZA OBCIĄŻEŃ GRANICZNYCH PODŁOŻA COULOMBA-MOHRA

S t r e s z c z e n i e

Podano przykłady przestrzennych mechanizmów plastycznej deformacji materiału Coulomba-Mohra. Przedstawione pola deformacji wykorzystano do obliczeń górnej oce-ny nośności fundamentów kwadratowych kinematyczną metodą analizy stanów granicz-nych. Problem obciążeń granicznych rozwiązano także metodą różnic skończonych. Obliczenia metodą numeryczną dały mniejsze wyniki niż analiza stanów granicznych. Dowodzi to, że dopuszczalne pola przestrzennej deformacji zbudowane z obszarów o lo-kalnie płaskim płynięciu są zbyt przybliżone i nie są odpowiednie dla praktyki inżynier-skiej. Metody, które poza warunkami brzegowymi nie wprowadzają ograniczeń na pole deformacji, są bardziej odpowiednim narzędziem inżynierskim do rozwiązywania prze-strzennych problemów nośności granicznej.

Received, 2002-02-04.